Table 20: Nominal cross sections

W range(GeV)	40-140	40.0-71.3	71.3-140.0
$\Delta F = F(y_2) - F(y_1)$	0.112	0.058	0.054
mean W^* (GeV)	74.8	53.4	99.9
nominal $\langle\epsilon\rangle$	0.35 ± 0.01	0.35 ± 0.01	0.35 ± 0.01
$N_{J/\psi}$	61 ± 11	28 ± 7	35 ± 8
$\sigma_{ep}(y_1, y_2)$ (nb)	6.0 ± 1.1	2.8 ± 0.7	3.4 ± 0.8
$\sigma_{\gamma p} = \frac{\sigma_{ep}}{\Delta F}$ (nb)	53 ± 10	47 ± 12	64 ± 15

7.7 Systematic errors

Systematic errors come from five sources.

1. Luminosity error. This error affects comparison of the cross sections measured by the ZEUS experiment and other experiments, but does not affect comparisons between the ZEUS results of different leptonic decay modes and different W regions.
2. $J/\psi \to e^+e^-$ branching ratio error. This error causes a little inconvenience in comparison of the cross sections measured by the ZEUS experiment and other experiments if different nominal branching ratio values are used.
3. Theoretical uncertainty. This is the error in the differential cross section $d\sigma/dx$. This error arises from incorrect modeling of the signal and background processes. For the signal process, this includes the uncertainty in the gluon distribution, t dependence of pomerons, and polarization of J/ψ. For background processes, this includes the uncertainty in the parameter n in $d\sigma/dM_x^2 \sim M_x^{-n}$ of the proton diffractive process. Theoretical uncertainty affects $\langle\epsilon\rangle$ determination.
4. Acceptance error. This is the error in local acceptance $\epsilon(x)$. This error is due to incorrect modeling of the detector and the beam conditions, e.g., discrepancy between the detector hardware and its simulation, such as calibration of the CAL energy scale and the CTD wire

positions, resolution of energy and position measurement, unnoticed changes of the calibrations over time, uranium noise in the CAL, unnoticed changes of beam conditions(vertex, beam-gas rate) and so on.

5. Background subtraction. This is the error in purity ρ. This error is a combination of theoretical uncertainty and systematic error in reconstruction of the invariant mass.

Systematic effects can be checked by varying parameters in doubt in their uncertainty ranges, or by using a different approach in data selection, or by applying the same processing procedure to different sub-sets of the data if the source of error is ambiguous.

Errors from various sources are listed in Table 21 in three categories.

□ *Luminosity and branching ratio errors*

Uncertainty of the integrated ep luminosity is 3%. $B(J/\psi \to e^+e^-)$ varies between 0.060 ± 0.002 and 0.063 ± 0.002 over the last few years.[70,12] An error of 4% is therefore assigned to this branching ratio. These lead to an overall normalization error of 5%.

□ *Theoretical uncertainty*

The distribution in $\cos\theta_{\text{decay}}$ in general follows $f(x;\alpha) = \frac{1+\alpha x^2}{2+2\alpha/3}$, where $x = \cos\theta_{\text{decay}}$. The acceptance as a function of α is derived as follows:

$$\begin{aligned}
\frac{\langle\epsilon(\alpha)\rangle}{\langle\epsilon(\alpha=0)\rangle} &= \frac{\int f(x;\alpha)\,\epsilon(x,y,t)\,dx d\sigma_{(y,t)}}{\int f(x;0)\,\epsilon(x,y,t)\,dx d\sigma_{(y,t)}} \\
&= \frac{\langle f(x;\alpha)\rangle_\epsilon}{\langle f(x;0)\rangle_\epsilon} \\
&= \frac{\langle \frac{1+\alpha x^2}{2+2\alpha/3}\rangle_\epsilon}{\frac{1}{2}} \\
&= \frac{1+\alpha\langle x^2\rangle_\epsilon}{1+\alpha/3} && (80) \\
&= \frac{1}{N_{\text{sel}}}\sum_{i=1}^{N_{\text{sel}}}\frac{1+\alpha x_i^2}{1+\alpha/3} && (81)
\end{aligned}$$

From EPJPSI MC data samples, it is found that $0.20 < \langle x^2 \rangle < 0.22$, and $\frac{\langle \epsilon(\alpha=1) \rangle}{\langle \epsilon(\alpha=0) \rangle} \approx 0.90$. From existing measurements, $\alpha < 0$ is unlikely. Average acceptance $\langle \epsilon \rangle$ was found to vary within 10% from that expected from geometrical acceptance between 35° and 145°(roughly corresponds to W = 40-140GeV cut).

Unlike the simple case of the decay lepton distribution where there is only one parameter α bounded between $(-1, 1)$, the distribution of J/ψ depends on several less constrained parameters. The transeverse distribution(in t) is approximately described by an exponential function with one parameter. The longitudinal distribution(in W) is sensitive to the gluon distribution. We evaluated the acceptance $\langle \epsilon \rangle$ according to four MC samples(see Figure 54). The model dependence is larger in the forward bin(W =40-71.3GeV), and may be as large as 10%. The theoretical uncertainty can not be evaluated accurately for two reasons, both are related to the low statistics of the real data sample. First, there is a statistical error of 3-4% in the MC data. Since the statistical error in the real data is more than 15%, there is no urgent need to increase the MC sample size for the 1993 data analysis. Secondly, parameters in the model(except α) are constrained only by the real data. However, the large statistical error in the real data prevents an accurate comparison of the real data and the MC data.

□ *Acceptance error*

CAL-FLT energy calibration affects event acceptance near the threshold. For this analysis, CAL_E with a threshold of 2GeV is the major source of error. The uncertainty was about 1 ADC count(about 0.2GeV) in the 1993 runs. By increasing CAL_E threshold by one ADC count for those events triggered by the GFLT $J\psi \to ee$ subtrigger only, the decrease in acceptance was found to be 6%.

In diffractive event selection, it was required that $E_{\mathrm{CAL}} - E_{e^+} - E_{e^-} - EMC_{DU} - HAC_{DU} < 1$GeV. As explained in Chapter V, EMC_{DU} and HAC_{DU} are energy sums over isolated EMC cells with energy below 80 MeV and isolated HAC cells with energy below 140 MeV respectively. EMC_{DU} and HAC_{DU} for several lower thresholds had been calculated and saved in the preselection ntuple for the real data and the MC data to study effects of noise suppression levels. By lowering

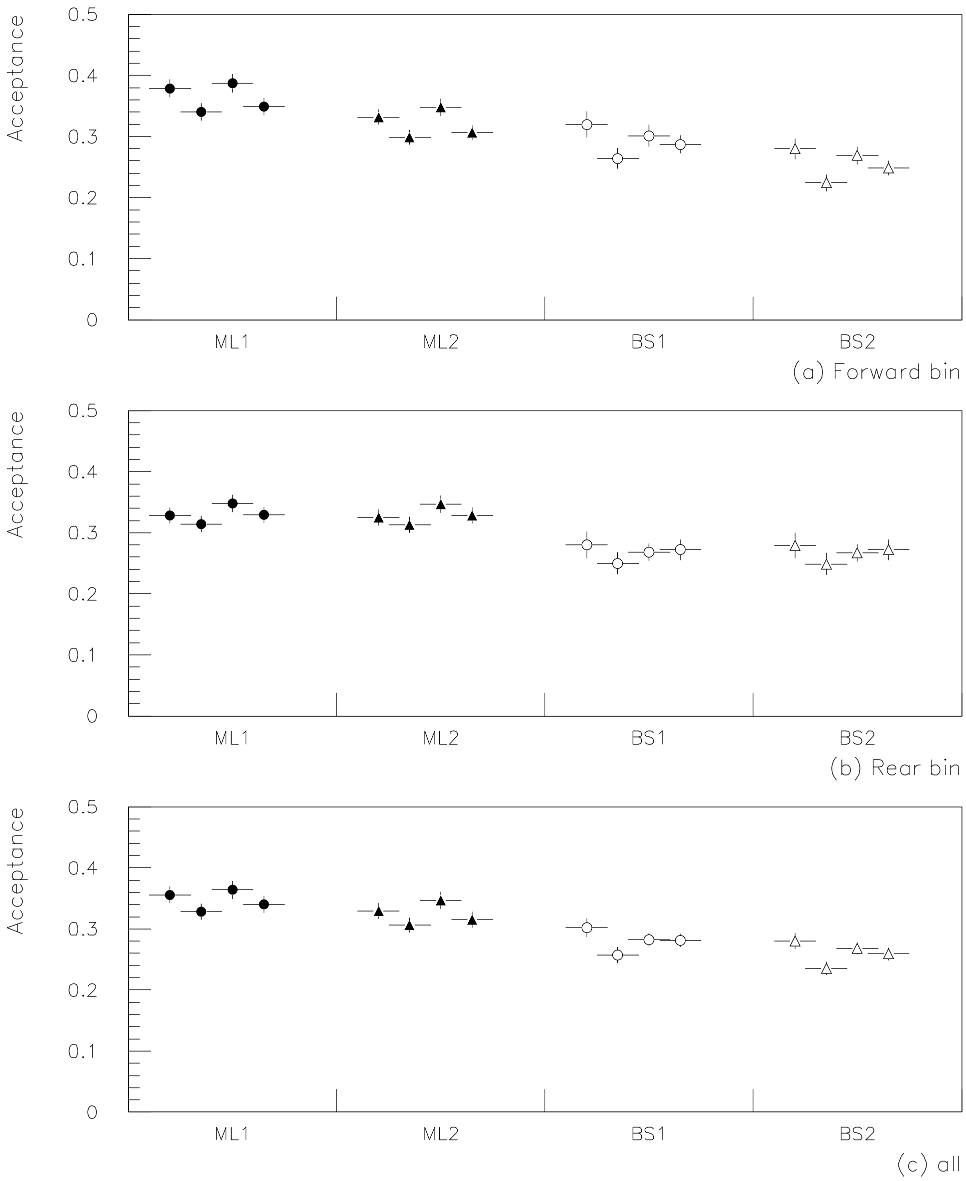

Figure 54: Model dependence of the average acceptance. Four MC samples are: EPJPSI11, EPJPSI12, EPJPSI13, DIPSI. Four methods are: ML1(ML with BGF05), ML2(ML irrespective of BGF05), BS1(BS with BGF05), BS2(BS irrespective of BGF05)

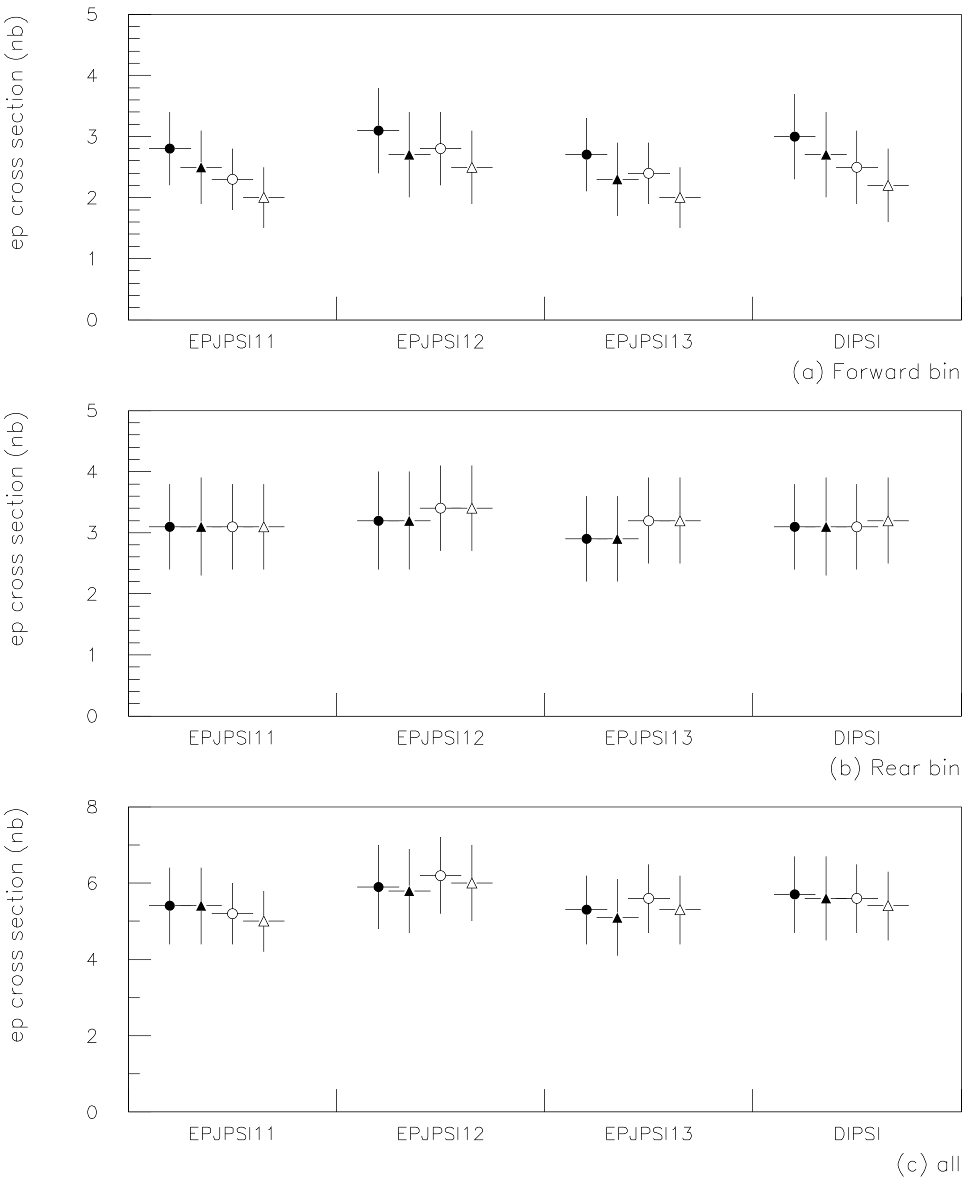

Figure 55: ep cross section determined by different methods. Four MC samples: EPJPSI11, EPJPSI12, EPJPSI13, DIPSI. Two TLT sets: with BGF05($\circ$) and irrespective of BGF05(Δ). Two background subtraction methods: ML(filled) and BS(empty).

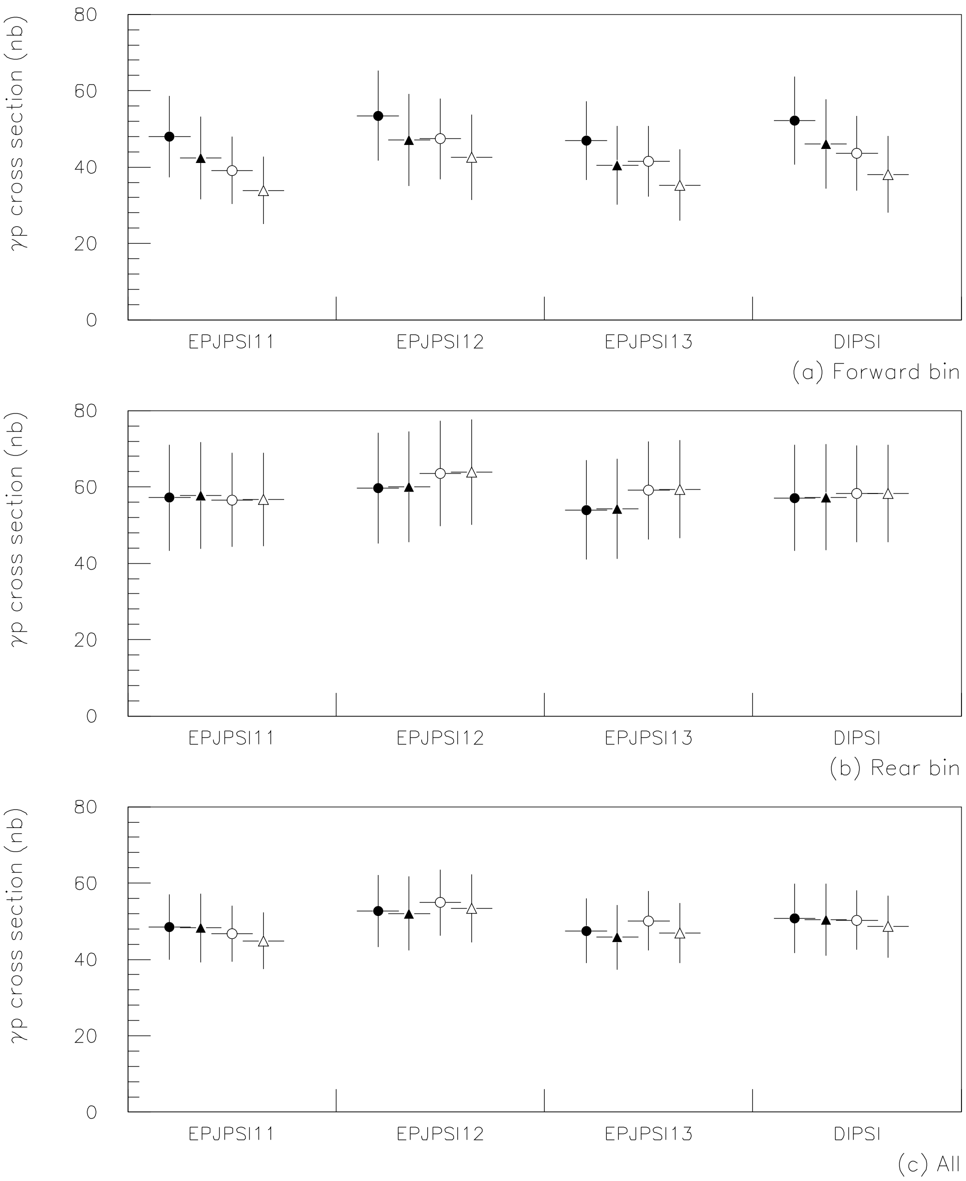

Figure 56: γp cross section determined by different methods. Four MC samples: EPJPSI11, EPJPSI12, EPJPSI13, DIPSI. Two TLT sets: with BGF05($\circ$) and irrespective of BGF05(Δ). Two background subtraction mothods: ML(filled) and BS(empty).

the noise energy thresholds in both MC and real data selection, the effect of this uncertainty was estimated to be 5%.

Results of systematic checks are shown in Figure 54, Figure 55 and Figure 56. In Figure 54, the $\langle \epsilon \rangle$ determined by different methods can be different even without systematic errors, but the difference between different MC models using the same method should agree if there were no systematic errors. The error bars in these figures are mainly statistical errors. Systematic errors are mostly hidden by the statistical errors. Although the acceptance of the TLT BGF05 filter was increased by nearly 50% in the October trigger configuration compared to the August trigger configuration, the difference in the cross section is not expected to be that large since there are large overlaps between BGF05 and the other two filters.

Errors from independent sources are added in quadrature. Theoretical uncertainty has a large contribution to the total systematic error.

Table 21: Systematic errors for the cross section measurement

uncertainty in	contribution to error
branching ratio	$\pm 4\%$
int. luminosity	$\pm 3\%$
J/ψ polarization	$\pm 5\%$
diffractive J/ψ model	$\pm 12\%$
inelastic J/ψ model	$\pm 3\%$
CAL noise suppression	$\pm 4\%$
FLT CAL_E threshold	$\pm 6\%$
Total	$\pm 16\%$